COMPUTATIONAL DESIGN OF BIOMIMETIC GELS WITH PROPERTIES OF HUMAN TISSUES

Y. Sliozberg*, J. Andzelm, J. K. Brennan, and M. VanLandingham
U. S. Army Research Laboratory
Aberdeen Proving Ground, MD 21005-5069

V. Pryamitsyn, V. Ganesan
Department of Chemical Engineering, University of Texas at Austin
Austin, Texas 78712

ABSTRACT

The effective design of body armor requires the use of biomimicking materials that accurately and robustly reproduce the characteristic mechanical behavior of human tissues. The mechanical performance of the soft tissues is determined by their viscoelastic properties and for this reason the optimal soft tissue surrogate must viscoelastically mimic the original tissue. One traditional tissue surrogate material is a water-based gelatin gel that has poor environmental stability and limited tailorability. Gel systems based on self-assembled, amphiphilic ABA triblock copolymers have similar properties to the gelatin system, forming the stable, spatially extended networks with a tunable viscoelastic behavior. In the present work, we have developed a systematic way to evaluate the viscoelastic properties of the biomimetic gels to control their mechanical properties. We have validated our approach using experimental data and demonstrated that our simulation results are in good qualitative agreement with the experimental data. The structure-property relationships found from the mesoscale simulation allows us to control mechanical properties of these gels in order to mimic a wide range of soft tissues. The viscoelastic properties have been calculated employing a non-equilibrium oscillatory shear technique used with the Dissipative Particle Dynamics method (DPD).

1. INTRODUCTION

The mechanical response of living tissue is crucial to identifying the potential injuries related to impact events. The U.S. Army still routinely uses gelatin as a standardized medium to test the terminal performance of firearms ammunition. Ballistic gelatin is a thermoreversible material composed of denatured collagen and when cooled lower than 30° C, it forms a gel consisting of the rigid triple helix zones interbridged by flexible coils. The ballistic gelatin approximately simulates the density and viscosity of human soft tissues and provides similar performance for most ballistics testing. The elastic modulus of ballistic gelatin is approximately equal to 100–150 kPa at a temperature near 10 ºC, and is comparable with the elastic modulus of soft tissue, which varies from 25 to 300 kPa. Low cost and availability are also major advantages of the ballistic gelatin.

However, the use of ballistic gelatin has several significant disadvantages. Variable molecular-weight distribution of naturally produced gelatin and procedural differences can lead to inconsistent mechanical properties and impede data analysis. The evaporation of water can also alter mechanical properties of the gelatin. Finally, as mentioned, the properties of ballistic gelatin only approximate soft tissue over a narrow temperature range around 10 °C, rapidly losing its solid-like consistency as temperature increases toward its gel temperature, 30 °C, at which point it becomes a liquid (Juliano et al., 2006).

Taking into account all these factors, the application of novel polymer surrogate systems for impact studies is needed to improve the repeatability and reproducibility of testing while providing robust model validation capabilities. Polymer gels based on blends of synthetic copolymers in a solvent exhibit improved thermal and environmental stability and possess tunable viscoelastic properties over a broad range of strain rates.

ABA triblock copolymers are one example of a polymer gel which has been widely used in many practical applications. ABA triblock copolymers undergo microphase separation in midblock-selective solvent and form a spatially extended network. The microstructure of this network depends on several factors such as temperature, copolymer concentration, block architecture, and relative length of the hydrophobic and hydrophilic blocks. The polymer network consists of physical cross-links comprising of the solvent-incompatible endblocks (micelles) connected by the midblocks (bridges). The micelles are surrounded by a corona consisting of midblocks (loops) formed as a result of close association of the endblocks (Fig. 1). The bridges act as active chains of the network and are treated as elastic springs, where loops do not contribute to the gel network elasticity (Drozdov et al., 2004; Tanaka, 2002). For that reason, bridge-to-loop ratio is one of the important factors defining the mechanical properties of a gel and this ratio depends on several factors such as copolymer concentration and the relative length of the blocks. The bridge to loop ratio increases with relative length of the

Report Documentation Page

Form Approved
OMB No. 0704-0188

1. REPORT DATE	2. REPORT TYPE	3. DATES COVERED
DEC 2008	**N/A**	**-**

4. TITLE AND SUBTITLE	5a. CONTRACT NUMBER
Computational Design Of Biomimetic Gels With Properties Of Human Tissues	5b. GRANT NUMBER
	5c. PROGRAM ELEMENT NUMBER
6. AUTHOR(S)	5d. PROJECT NUMBER
	5e. TASK NUMBER
	5f. WORK UNIT NUMBER
7. PERFORMING ORGANIZATION NAME(S) AND ADDRESS(ES) **U.S. Army Research Laboratory Aberdeen Proving Ground, MD**	8. PERFORMING ORGANIZATION REPORT NUMBER
9. SPONSORING/MONITORING AGENCY NAME(S) AND ADDRESS(ES)	10. SPONSOR/MONITOR'S ACRONYM(S)
	11. SPONSOR/MONITOR'S REPORT NUMBER(S)

12. DISTRIBUTION/AVAILABILITY STATEMENT
Approved for public release, distribution unlimited

13. SUPPLEMENTARY NOTES
See also ADM002187. Proceedings of the Army Science Conference (26th) Held in Orlando, Florida on 1-4 December 2008, The original document contains color images.

14. ABSTRACT

15. SUBJECT TERMS

16. SECURITY CLASSIFICATION OF:			17. LIMITATION OF ABSTRACT	18. NUMBER OF PAGES	19a. NAME OF RESPONSIBLE PERSON
a. REPORT	b. ABSTRACT	c. THIS PAGE			
unclassified	**unclassified**	**unclassified**	**UU**	**8**	

midblock with respect to the length of the endblocks and copolymer concentration (Shen et al., 2007; Szczubiałka et al., 2000).

In this study, we attempt to create, through computational modeling, a predictive tool that answers questions regarding the impact of chemical and compositional variables on the viscoelastic properties. Understanding such structure-property relationships will enable the development of biomimetic gels that mimic a wide range of soft tissues over a wide range of strain rate.

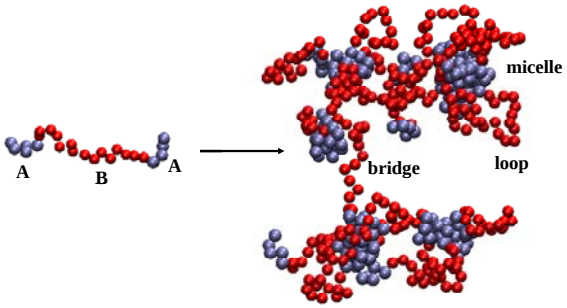

Fig. 1. Schematic representation of a polymer network formed from ABA triblock copolymer.

2. MODEL AND SIMULATION METHODS

Generally speaking, atomistic molecular dynamics is suitable up to 100 nanometers and several nanoseconds, which makes it difficult to perform simulations of large polymeric system on comparable timescales. In this study, we have exploited the Dissipative Particle Dynamics (DPD) simulation technique which consists of coarse-grained particles that represent molecular clusters rather than individual atoms. The DPD method is a mesoscale simulation technique that operates at time and length scales larger than those of traditional molecular dynamics, but for situations that are still inaccessible at the continuum level.

2.1 Coarse-Grained Model of $A_1B_xA_1$ Triblock Copolymer

The three-dimensional system consists of N_t DPD particles of triblock copolymers plus solvent confined in a cubic domain with periodic boundaries in all directions. The system has N chains of $A_1B_xA_1$ triblock copolymer composed of particles of types "A" and "B" of total length M immersed in a midblock-selective solvent whose particles are of type "S." Each DPD bead represents roughly the same volume. Each chain has two endblocks represented by a single bead of type "A" and a midblock composed of x particles of type "B" (Fig. 2). The number of triblock chains is chosen from

$$N = \frac{cN_t}{M}, \qquad (1)$$

where $M = x + 2$ and c is a volume fraction of the triblock in the solution. It is important to mention that we model an endblock of any size as a single bead to avoid its collapse to a smaller size before the association with the other endblocks takes place.

The physical size of the interaction radius for the DPD particle, R_c depends on the molar volume of the endblock and may be estimated from

$$R_c = \sqrt[3]{\frac{\rho v_A}{N_A}}, \qquad (2)$$

where ρ is the DPD bead density, v_A is the molar volume of the endblock, and N_A is Avogadro's Number. x is evaluated from the volume fracture of the end block in the dry copolymer, f_A.

$$x = \frac{2(1 - f_A)}{f_A}. \qquad (3)$$

Note that, because the endblock of any length is represented by one DPD bead, x corresponds to the relative length of the middlebock in the triblock copolymer.

The poly(styrene-block-isoprene-block-styrene) copolymer or SIS in the I-selective solvent has been chosen as a model triblock copolymer for this study because of its promising properties as a biomimetic gel and sufficient amount of existing experimental structural and rheological data to validate our model.

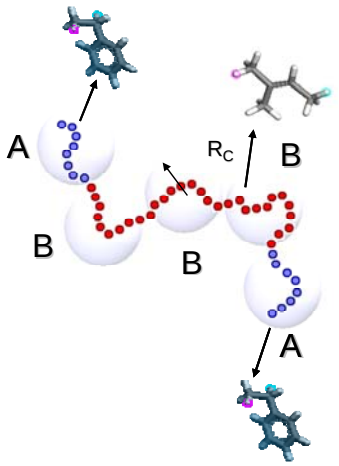

Fig. 2. Schematic representation of $A_1B_3A_1$ triblock copolymer mapped on DPD model. Poly(styrene-block-isoprene-block-styrene) copolymer is chosen as an example.

2.2 Dissipative Particle Dynamics

A DPD system is composed of soft particles, each representing a region of fluid, which moves according to Newton's equations of motion continuously in space and discreetly in time. In a DPD simulation, the polymer chain is modeled as a collection of point particles that represent lumps of the chain containing several segments. Force acting on DPD particles, F is written as the sum of a conservative force F^C, dissipative force F^D, and random force F^R:

$$\mathrm{F_{ij}} = \mathrm{F_{ij}^{C}} + \mathrm{F_{ij}^{D}} + \mathrm{F_{ij}^{R}} \,. \qquad (4)$$

F^C includes a soft repulsion force F^{Cr} acting between two particles and a harmonic spring force F^{Cs} acting between adjacent particles in a polymer chain. F^{Cr} and F^{Cs} are given by

$$\mathrm{F_{ij}^{Cr}} = \begin{cases} \mathrm{a_{ij}}\left(1-\dfrac{\mathrm{r_{ij}}}{\mathrm{r_c}}\right)\dfrac{\mathrm{r_{ij}}}{\mathrm{r_{ij}}} & \text{for } \mathrm{r_{ij}} < \mathrm{r_c} \\ 0 & \text{for } \mathrm{r_{ij}} \geq \mathrm{r_c} \end{cases} \qquad (5)$$

and

$$\mathrm{F_{ij}^{Cs}} = -\mathrm{K}\left(\mathrm{r_{ij}} - \mathrm{r_0}\right)\frac{\mathrm{r_{ij}}}{\mathrm{r_{ij}}} \,, \qquad (6)$$

respectively.

In Eq. 5 and 6, a_{ij} is the maximum repulsion between particle i and particle j, $\mathrm{r_{ij}} = \mathrm{r_i} - \mathrm{r_j}$, $\mathrm{r_{ij}} = \left|\mathrm{r_{ij}}\right|$, $\mathrm{r_c}$ $\mathrm{r_c}$ is the cutoff radius, K is the spring constant, and r_0 is the equilibrium spring length. The evolution of DPD particles in time t is governed by Newton's equations of motion. For a more detailed description, see the original papers (Hoogerbrugge and Koelman, 1992; Koelman and Hoogerbrugge, 1993).

2.3 Viscoelastic Property Calculations

When a linear viscoelastic material is subjected to oscillatory strains, γ, of frequency ω, the stress response, σ, is necessarily cyclic and can be written, as: $\sigma(\omega) = A_{\omega}(G'(\omega)\sin(\omega t) + G''(\omega)\cos(\omega t))$. The storage modulus, G', indicates the material's ability to store energy and the loss modulus, $G''(\omega)$ characterizes the amount of energy lost through the viscous process.

Simulations can be used to determine which parameters govern the viscoelastic behavior of polymer systems, delineating the regimes and frequencies at which various effects (e.g., polymer chain length) are manifested. The viscoelastic properties are calculated using a non-equilibrium oscillatory shear technique (Pryamitsyn and Ganesan, 2006), which entails a simulation with an additional force in the shear direction along with time-dependent Lees-Edwards boundary conditions (Lees and Edwards, 1972). For oscillatory shear imposed in the x-y plane, the equation of motion for the particle velocities becomes

$$m_i \frac{dv_{ix}}{dt} = f_{ix} + m_i r_{iy} \frac{d^2\gamma(t)}{dt^2} \qquad (7)$$

The oscillatory strain can be taken as $\gamma(t) = A_{\omega}\left[1-\cos(\omega t)\right]$, where A_{ω} and ω are the chosen values of the amplitude and frequency, respectively.

2.4 Simulation Parameters

DPD reduced units system are adopted for the convenient expression of parameters and are taken as: length in R_c, energy in k_BT/R_C, mass in particle mass m, and time in $\tau = R_c\sqrt{m/k_BT}$ (Groot and Rabone, 2001). Therefore, the physical value of moduli are calculated from

$$G = G_{DPD}k_BT/\left(R_c\right)^3, \qquad (8)$$

where T is the temperature and k_B is Boltzmann's constant. We choose $m=k_BT=R_C=1$, time step $\Delta\tau=0.02$, and overall particle density $\rho=3$. K and r_o in Eq. 6 for the triblock are 1 and 3, respectively.

The repulsive parameters for like particles a_{ii} are determined from the value of the dimensionless compressibility (Groot and Warren, 1997): $k^{-1} \approx 1 + 0.2a_{ii}/\rho T$, where k^{-1} is given by

$$k^{-1} = \frac{1}{nk_BTk_T} \qquad (9)$$

and where k_T is the isothermal compressibility and n is the number density. a_{ii} is taken as 25 for water, while for organic solvent composed of larger-size molecules we estimated a_{ii} to be 50.

The repulsive parameters for unlike partciles a_{ij} are determined according to the linear relation with Flory-Huggins parameters (Groot and Warren, 1997):

$$a_{ij} \approx a_{ii} + 3.27\chi_{ij} \qquad (10)$$

where χ_{ij} parameters are mapped from the real polymers to the short simulated chains preserving $\chi M = const$.

For our model block copolymer system SIS in an organic solvent, the interaction parameter for the polystyrene-polyisoprene, $\chi_{PS\text{-}PI}$ has been taken from the literature, equal to 0.086 for 30° C for M = 432. Interaction parameter between endblock and solvent is chosen such that $\chi M \geq 50$ to ensure good segregation. The maximum repulsive force a_{ij} is calculated according to Eq. 10 and given in Table 1.

Table 1. Repulsive parameters between a pair of DPD particles.

DPD pair	S-S	A-A	B-B	A-B	A-S	B-S
a_{ij}	50.0	50.0	50.0	66.0	105.0	50.0

2.5 Methodology

In this study, we have investigated the role of relative block size and concentration of triblock copolymer on the structure and structure-related mechanical properties of formed polymeric gels. In order to validate our method we choose $A_1B_6A_1$ in B selective solvent as a prototype of SIS of molecular weight (7.2-35.8-7.2 kg/mol) in the I-selective solvent, *n*-tetradecane studied by Watanabe et al. (Watanabe et al., 2000) using methodology described in Section 2.1. We choose concentration of $A_1B_6A_1$ 0.2, 0.3, 0.4, and 0.5 wt, which correspond to the volume fraction, c equal to 0.17, 0.28, 0.39, and 0.50. The triblock would adopt micellar morphology for the room temperature for this concentration range. In order to probe effect of relative block length, we consider x equal to 3, 6, 9, 12, 15, and 18.

We have performed the equilibrium simulation of the system consisted of randomly generated polymer chains and solvent particles slowly adjusting the periodic box size to the desired pressure followed by a constant temperature annealing simulation. This procedure has been repeated six times verifying that the system pressure does not change as an indication of an equilibrium state. Ten parallel simulation runs were issued for each set of initial conditions. We examined the microstructure of each equilibrium state to determine the conformation of each midblock in the gel using the following micelle-identifying algorithm. The midblock is considered to be in a loop conformation if both endblocks belong to the same micelle. If the midblock connects two different micelles it is considered to be in a bridge conformation. An unassociated endblock can also form a dangling tail conformation for the midblock. Visual inspection of the microstructure was also performed.

Following equilibration of the structure, a series of stress trajectories are generated by imposing the oscillatory shear conditions with 0.1% strain. Since the DPD simulation is generally able to access only frequencies in the megahertz regime, dynamic moduli have been linear extrapolated. Note that numerical errors tend to be higher at low frequencies requiring averaging over more stress trajectories to minimize these errors, which is ineffective and leads to very long simulation times. This suggests that a new computational approach to estimating the mechanical properties of ABA triblock copolymer is needed.

3. RESULTS AND DISCUSSION

3.1. Validation of our method.

For the validation purposes, we have compared the microstructure and the mechanical properties of our gel to experiment (Watanabe et al., 2000). All simulation runs resulted in microphase separation which led to a three-dimensional network structure of a micellar gel with the middle block exhibiting bridge or loop conformations. Fig. 3. shows an example of an equilibrated system.

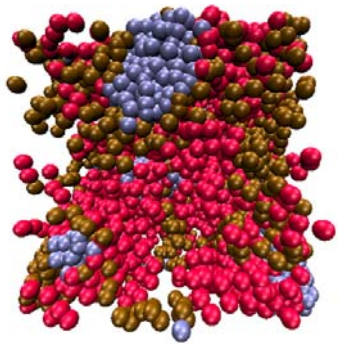

Fig. 3. Equilibrated structure of DPD simulation of $A_1B_9A_1$ copolymer. Micelles comprised of type "A" particles are shown in blue. The bridge and loop conformations of the middle blocks are shown as red and brown, respectively. Solvent particles are not shown.

Fig. 4 compares the estimated loop fractions of the middle block from the DPD simulation (b), with those obtained by Watanabe et al. by measuring the dielectric losses of the SIS in *n*-tetradecane (a). Simulation results are in good qualitative agreement with the experimental data.

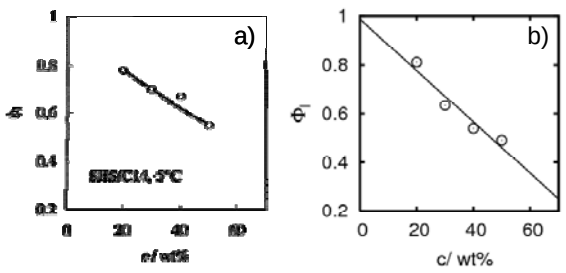

Fig. 4. Loop fraction as a function of copolymer concentration (a) for SIIS (7.2-17.9-17.9-7.2)/C14 (Watanabe et al., 2000) (b) from mesoscale simulation of $A_1B_6A_1$ triblock copolymer.

The storage modulus, *G´* obtained by our simulations exhibits quite extensive behavior with a numerical value close to a plateau for accessible DPD frequencies. We do not consider the loss modulus *G"(ω)* is this study because its value is prone to numerical error of calculation. The equilibrium value of storage modulus, *G* found from DPD simulation has been mapped back to its physical value using Eq. 8. Table 2 shows the simulated and experimental rheological data and demonstrates relatively accurate representation of experimental data with DPD simulation. Note that because the I blocks in the SIS solutions are not entangled due their low molecular weight ($M_w \approx 50000$), DPD simulation results are in a good agreement with experimental data.

Table 2. Comparison between equilibrium values of shear modulus estimated from simulation, G_{sim} and obtained from experimental data, G_{exp}

conc.,wt	0.2	0.3	0.4	0.5
$\log(G_{sim})$	3.29	3.79	3.95	4.11
$\log(G_{exp})$	2.70	3.40	3.85	4.20

3.2 Governing Equation for Elastic Shear Modulus

Gels are characterized by a storage modulus, *G´* that often is only weakly dependent on frequency, ω over a broad range and is several order of magnitude larger than the loss modulus, *G"(ω)*. Thus, elastic response appears to be a reasonable assumption, such that the equilibrium storage modulus, *G* is given by

$$G = \rho\left(\nu_b G_b + \nu_l G_l + \nu_t G_t\right) \qquad (11)$$

where ρ is copolymer density, ν_b, ν_l and ν_t are number density of bridges, tail and dangling tails and G_b, G_l and G_t are the elastic modulus of a single bridge, loop or dangling tail respectively.

For the strong separation condition we can assume that the contribution of tails is negligible and that all midblocks have either bridge or loop conformation. Using Eq. 1 and evaluating number of bridges, N_b as $N_b = N\phi_b(x,c)$ and number of loops, N_l as $N_b = N\left(1-\phi_b(x,c)\right)$ we get the equilibrium elastic modulus as:

$$G = \rho\frac{c}{x+2}\left[G_b\phi_b(x,c) + G_l\left(1-\phi_b(x,c)\right)\right] \qquad (12)$$

for $\chi M > 50$, where $\phi_b(x,c)$ is bridge fraction, that is a function of the relative block size and copolymer concentration.

3.3 Fraction of Bridges

To compare effect of concentration and relative block size on fraction of bridges, ϕ_b we have performed a set of simulations with variable concentration, *c* and length of the midblock, *x*. We present our results in Fig. 5. From this figure, one can see that ϕ_b increases with increasing of the copolymer concentration. ϕ_b increases with increasing of the relative length of the middle block for the shorter middle blocks ($x < 9$). For the relatively long middle block compared with the endblock ($x \geq 9$), ϕ_b only weakly depends on the middle block length. This behavior is especially pronounced for low concentration ($c = 0.2$), where $\phi_b \approx 0.4$ for all $x \geq 9$. This is a result of the lower probability for the endblocks of the different copolymer chains in a dilute triblock solution to form a network since close association is minimized.

The compact size of the middle block compared to the distance between aggregates leads to the tendency to form loops. For example, for $x = 3$, all middle blocks form loops for the entire concentration range. Increasing the copolymer concentration increases the probability of each chain developing a bridge such that ϕ_b reaches a maximum value, $\phi_b^{\max}$ for the the pure copolymer. For the reasonable degrees of incompatibility $\chi M \geq 100$ corresponding to the relatively long midblock ($x \geq 9$) $\phi_b^{\max}$ is approximately 0.66. This value is in good agreement with theoretical work (Jones et al., 1996) having $\phi_b^{\max}$ equal to 0.63.

For relatively high degree of incompatibility ($\chi M \geq 50$), ϕ_b is only a function of concentration and triblock architecture. However, in general, ϕ_b also depends on degree of incompatibility or $\phi_b = f\left(c, x, \chi M\right)$. This dependence becomes significant for endblocks with a low degree of polymerization in a non-highly selective

solvent. For this case, the number of unassociated endblocks would be higher and both ϕ_b and ϕ_l would have smaller values. To address this situation we can change the repulsive parameters in our model according to Section 2.4 and then evaluate ϕ_b. It is important to mention that ϕ_b does not depend on the absolute length of the blocks but depends on the relative block sizes.

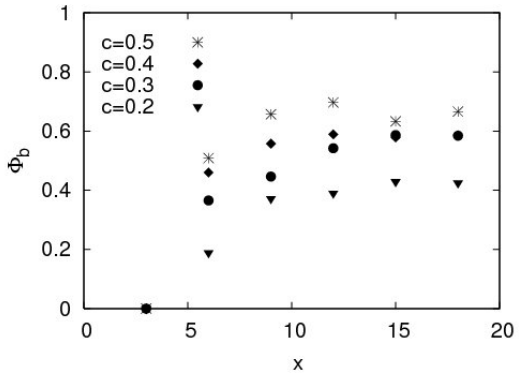

Fig. 5. Fraction of bridges for $A_1B_xA_1$ copolymer as a function of the relative block size at the various concentrations.

3.4 Elastic Shear Modulus

To assess the effect of concentration and relative block size on the equilibrium elastic modulus, *G* we have performed oscillatory shear simulations for the same set of concentration and length of the middle block we used for calculation of number of bridges. Results of shear simulations for $A_1B_{15}A_1$ are shown in Fig. 6.

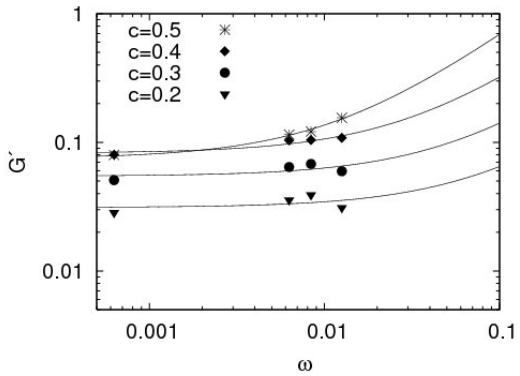

Fig. 6. Storage modulus for $A_1B_{15}A_1$ triblock copolymer as a function of frequency at various concentrations.

Following the procedure described earlier, we obtained *G* for various concentrations and lengths of the midblocks, and results are presented in Fig. 7. Since the midblock of $A_1B_3A_1$ forms only loops we can estimate the elastic modulus of a single loop to the elastic modulus, G_l from Eq. 12 setting ϕ_b equal to 0. Assuming that G_l does not change with concentration and the polymer length we found that $G_l \approx 0.114$ in DPD units. Having this value, we are able to find from Eq. 12 that the elastic modulus of a single bridge, G_b for the relative long middle block ($x \geq 9$) does not depend on concentration and block length and equal $G_b \approx 1.717$. For the shorter middle block ($x = 6$) $G_b \approx 0.995$ in DPD units. From these values, we conclude that contribution of the loops compared to the bridges to the elastic modulus is negligible.

From entropic elasticity theory (Ferry, 1980), the contribution of one bridge to the equilibrium elastic modulus is estimated as

$$G_b = \mu k_B T\,, \qquad (13)$$

where μ is a coefficient of order of unity. Thus, we have found that $\mu \approx 1.717$ for $x \geq 9$.

Mapping our results to physical values of the elastic modulus for the ABA triblock copolymer and having specified ρ=3, we can finally write

$$G = \frac{1.717RT}{v_A(x+2)} c\phi_b(x, c, \chi M), \qquad (14)$$

where *R* is the universal gas and $x \geq 9$. In Eq. 14 the volume fraction, *c*, the molar volume of A block, v_A and degree of incompatibility χM characterize the physical triblock copolymer and solvent. The relative size of the midblock with respect to the endblock, *x*, is evaluated from Eq. 3. Corresponding to these parameters, the fraction of bridges $\phi_b(x, c, \chi M)$ is determined from equilibrium DPD simulation. Eq. 14 (solid lines in Fig. 7) is applicable for the relative long midblock compared to the endblock size ($x \geq 9$). For $x < 9$, we found the coefficient, μ, being less 1.717, for example approximately 1.0 for $x = 6$.

Because ϕ_b increases with increasing relative length of the middle block for $x < 9$ and only weakly depends on the middle block length for $x \geq 9$, the elastic modulus for each concentration has a maximum value and then decreases with increasing *x* (Fig. 7). According to Eq. 14, the elastic modulus increases with concentration directly and indirectly since ϕ_b is also increasing with concentration.

The main advantage of our model is that it can estimate the elastic response of ABA triblock copolymers of low molecular weight in a midblock-selective solvent directly from equilibrium DPD simulations

evaluating $\phi_b(x, c, \chi M)$. Since non-equilibrium shear simulation is not necessary, this approach greatly reduces the simulation time.

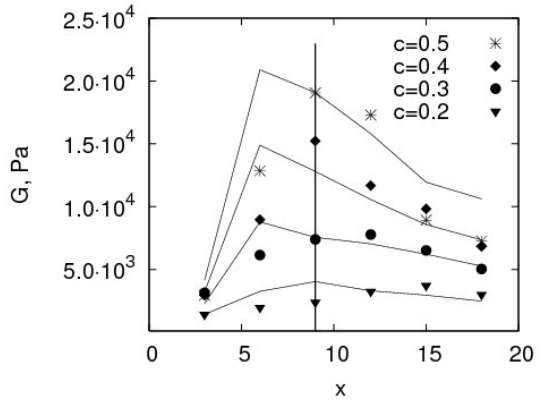

Fig. 7. Elastic modulus for $A_1B_xA_1$ as a function of the relative block size at various concentrations. Simulation data are represented with points and solid lines are fit to Eq. 14.Vertical lines show the applicable part of our model.

Eq. 14 is valid only for block copolymer of relatively low molecular weight where entanglement does not likely occur. For copolymers with higher molecular weight, entanglements and attractive interactions inside the micelles would give rise to a large additional contribution to the elastic modulus and the value of *G* would be an order of magnitude higher than one predicted with Eq. (14). To address this situation we propose to use a coefficient depending on the molecular weight, M_w and chemical composition, *q* of triblock copolymer: $p(M_w, q)$. For this case, Eq. 14 becomes

$$G = \frac{p(M_w, q)RT}{v_A(x+2)} c\phi_b(x, c, \chi M) \qquad (15)$$

where $p(M_w, q)$ has to be evaluated for each kind of ABA block copolymer by comparing simulation and experimental results.

To verify this approach, we have considered an example of a gel composed of SIS with higher molecular weight (M_w = 260 000) (Laurer et al., 1999). According to Eq. 15, with all parameters constant and only changing the volume fraction of SIS from 0.16 to 0.33 (micellar regime) will make the equilibrium elastic modulus should double. In Laurer's paper, *G* increases from 4000 to 9000 Pa making *G* 2.25 times higher for *c* changes from 0.16 to 0.33 (density of styrene and isoprene blocks are taken to be 1.04 and 0.913 g/cm^3, respectively).

For the second example, we have considered a blend of diblock and triblock copolymers of different relative block size (one gel contain 15 % by mass polysterene, PS-15 and the other gel contains 30 % by mass polysterene, PS-30) studied by Juliano et al. (Juliano et al., 2006). They observed that the elastic modulus does not significantly change from PS-15 to PS-30: $G_{PS-30}/G_{PS-15} = 1.17$. In this case, we can assume that the gel is mostly composed of triblock (80 % by mass) and evaluate *x* that equals 5.3 and 13 for PS-15 and PS-30. Assuming that changes in v_A and χM are negligible and taking value of $\phi_b(x, c)$ from our simulation, we can estimate from Eq. 15 that $G_{PS-30}/G_{PS-15} = 1.02$.

These two examples confirm that our approach can predict, with reasonable accuracy, the relative change of elastic modulus of a micellar gel composed of triblock copolymer of high molecular weight with changing polymer concentration, relative length of the blocks, solvent parameters, and temperature.

4. CONCLUSIONS

The equilibrium and non-equilibrium oscillatory-shear DPD simulation methods have been used for mesoscale simulation of gel-forming ABA triblock copolymer in a midblock-selective solvent. We have validated our approach using experimental data demonstrating that the result of our simulation results are in good qualitative agreement with the experimental data. We have developed a model that estimates the absolute value of the elastic response of ABA triblock copolymer of low molecular weight in a B-block selective solvent with high segregation regime ($\chi M \geq 50$) directly from equilibrium DPD simulation. This approach eliminates the necessity of computationally-costly non-equilibrium shear simulations.

We have demonstrated that our model can predict, with reasonable accuracy, the relative change of the elastic modulus of a gel consisting of triblock copolymer with changing polymer concentration, relative length of the blocks, solvent parameters, and temperature. This relationship, derived from the mesoscale simulation, will help us to reduce the time and effort necessary to set up experiments and eventually to control mechanical properties of ABA triblock copolymer gels in order to mimic a wide range of soft tissues.

According to our results, we can predict that the equilibrium elastic modulus of ABA triblock copolymer of low molecular weight would be at its low range for the relative short midblock compared with the endblock (more than 45 % by mass of styrene in dry copolymer that corresponds to $x < 3$) for any volume fraction of copolymer, *c* less than 0.5. For the lower styrene content

the elastic modulus does not significantly change with relative block size, and weakly decreases with decreasing styrene content after a maximum around 25 % ($x = 7$) of styrene in dry copolymer for the low copolymer content ($c \leq 0.2$). For the higher copolymer concentration ($c > 0.2$) the elastic modulus has a pronounced maximum around 25 % of styrene in dry copolymer.

All of these observations are valid for a highly selective solvent with respect to the midblock. For the endblocks with low degree of polymerization in non-highly selective solvent, the equilibrium elastic modulus has its maximum shifted to higher content of polysterene and its value drops significantly when the degree of incompatibility χM is less than 20. The position of this maximum should be evaluated for each particular solvent from the equilibrium DPD simulation.

According to our predictions we may extend our observations to the ABA copolymers with higher molecular weight including a large additional contribution of entanglements and attractive interactions inside the micelles to the equilibrium elastic modulus. However, to predict the rheology of copolymers with higher molecular weight more accurately, we propose to allow entanglements to occur in the DPD simulation (Goujon et al., 2008) or to exploit the "Sliplink" models for block copolymers (Masubuchi et al., 2006).

ACKNOWLEDGMENTS

This research was supported in part by an appointment to the Postgraduate Research Participation Program at the U.S. Army Laboratory administered by the Oak Ridge Institute of Science and Education through interagency agreement between the U.S. Department of Energy and USARL.

REFERENCES

Drozdov, A. D., Agarwal, S., and Gupta, R.K., 2005: The Effect of Temperature on the Viscoelastic Response of Polymer Melts, *Int. J. Eng. Sci.*, **43** 304-320.

Ferry, J. D. *Viscoelastic Properties of Polymers*; John Wiley & Sons, Inc.: Hoboken, NJ, 1980.

Goujon, F., Malfreyt, P., and Tildesley, D. J., 2008: Mesoscopic Simulation of Entanglements Using Dissipative Particle Dynamics: Application to polymer brushes, *J. Chem. Phys*., **129**

Groot, R. D. and Rabone, K. L., 2001: Mesoscopic Simulation of Cell Membrane Damage, Morphology Change and Rupture by Nonionic Surfactants, *Biophys. J.*, **61**, 725-736.

Groot, R. D. and Warren, P. B., 1997: Dissipative Particle Dynamics: Bridging the Gap between Atomistic and Mesoscopic Simulation, *J. Chem. Phys.*, **107**, 4423-4435.

Hoogerbrugge, P. J. and Koelman, J. M. V. A., 1992: Simulating Microscopic Hydrodynamic Phenomena with Dissipative Particle Dynamics.,*Europhys. Lett*., **19**, 155-160.

Juliano, T. F., Forster, A.M., Drzal, P. L., Weerasooriya, T., Moy, P., and VanLandingham, M. R., 2006: Multiscale Mechanical Characterization of Biomimetic Physically Associating Gels, *J. Mater. Res*., **21**, 2084-2092.

Jones, R. L., Kane, L., and Spontak, R. J. 1996: Morphological Characteristics of Lamellar ABA Triblock Copolymers: A Self-Consistent Field Treatment, *Chem. Eng. Sci.,* **51,** 1365-1375.

Koelman, J.M.V.A and Hoogerbrugge, P. J., 1993: Dynamic Simulations of Hard-Sphere Suspensions under Steady Shear, *Europhys. Lett*., **21**, 363-368.

Laurer, J. H., Khan, S. A., and Spontak, R. J., 1999: Morphology and Rheology of SIS and SEPS Triblock Copolymers in the Presence of a Midblock-Selective Solvent, *Langmuir*, **15**, 7947-7955.

Lees, A. W. and Edwards, S.F., 1972: The Computer Study of Transport Processes under Extreme Conditions, *Solid State Phys*., **5**, 1921-1929.

Masubuchi, Y., Ianniruberto, G., Greco, F., and Marrucci, G., 2006: Primitive Chain Network Model for Block Copolymers, *J. Non-Cryst. Solids*, **352**, 5001-5007.

Pryamitsyn, V. and Ganesan, V., 2006: Origins of Linear Viscoelastic Behavior of Polymer Nanoparticle Composites, *Macromolecule*, **39**, 844-856.

Shen, W., Kornfield, J., and Tirrell, D., 2007: Structure and Mechanical Properties of Artificial Protein Hydrogels Assembled through Aggregation of Leucine Zipper Peptide Domains, *Soft Matter*, **3**, 99-107.

Szczubiałka, K., Ishikawa, K., and Morishima, Y., 2000: Associating Behavior of Sulfonated Polyisoprene Block Copolymers with Short Polystyrene Blocks at Both Chain Ends, *Langmuir*, **16**, 2083-2092.

Tanaka, F., 2002: Intramolecular Micelles and Intermolecular Crosslinks in Thermoreversible Gels of Associating Polymers, *J. Non-Cryst. Solids*, **307-310**, 688-697.

Watanabe, H., Sato, T., and Osaki, K., 2000: Concentration Dependence of Loop Graction in Styrene-Isoprene-Styrene Triblock Copolymer Solutions and Sorresponding Changes in Equilibrium Elasticity, *Macromolecules*, **33**, 2545-2550.